Sixth International Symposium on Cavitation
CAV2006, Wageningen, The Netherlands, September 2006

EFFECT OF CAVITATION ON THE STRUCTURE OF THE BOUNDARY LAYER IN THE WAKE OF A PARTIAL CAVITY

Sarraf Christophe Institut de Recherche de l'Ecole navale (IRENav)
Ait Bouziad Yousef Laboratoire de Machines Hydrauliques, Ecole Polytechnique de Lausanne (LMH)
Djeridi Henda Institut de Recherche de l'Ecole navale (IRENav)
Farhat Mohamed Laboratoire de Machines Hydrauliques, Ecole Polytechnique de Lausanne (LMH)
Deniset François Institut de Recherche de l'Ecole navale (IRENav)
Billard Jean-Yves Institut de Recherche de l'Ecole navale (IRENav)

ABSTRACT

This study investigates the modifications of the turbulent boundary layer that develops on the suction side of a NACA0015 hydrofoil when a stable partial cavity takes place near the leading edge of the foil. The velocity field measured in non cavitating conditions has been compared with its equivalent in cavitating conditions. A particular focus has been put on the evolution of the logarithmic law of the velocity profile and on the modification of the global parameters that can precise both the position of the laminar-turbulent transition and the detachment of the boundary layer. The wall friction has been estimated both by use of a numerical procedure and by treatment of the experimental results. This comparison is encouraging and gives confidence in the proposed methodology.

The results have shown that the vapour phase modify the boundary layer thickness and enhance the exchanges with the external layer that lead to an increase of the velocity close to the wall. This phenomenon induces a stabilisation of the boundary layer and delays its separation.

INTRODUCTION

Cavitation is a significant engineering phenomenon that occurs in fluid machinery, variety boundary layer flows or liquid jet. A considerable effort has been realized to understand the fundamental physics of cavitation phenomena concerning the growth and collapse of individual bubbles near rigid boundaries or inception and development of sheet cavities. On hydrofoils at moderate angle of attack, bounded wall cavity appears on the suction side at the leading edge of the foil and many studies have analysed the behaviour of the cavity itself (Leroux *et al*., 2004). The evolution of the geometry of the cavity has been studied by many authors, the transition between stable and unstable behaviour of the cavity has been studied both experimentally and numerically, the conditions that prevail at the cavity closure have been studied and a large amount of information exists in the scientific literature and some descriptive work has been done on the boundary layer to describe the conditions that prevail at the opening of the cavity.

Works on sheet cavities conducted by Arakeri and Acosta (1973), Gates and Acosta (1978) or Katz (1984), have shown that in a boundary layer subjected to laminar separation the sheet cavity can be stabilized by the separated bubble. They showed that "band type cavitation" occurred as free stream bubbles were entrained into the separation region through the reattachment zone, where they were pushed upstream by the reverse flow. They provided for the first time a clue on the process of sheet formation but unanswered the questions relative to occurrence of the sheet cavity on surfaces without laminar separation. Franc and Michel (1985) provided a strong connection between cavitation and laminar separation of the boundary layer on a curved wall by dye injection at the leading edge of the body and they showed that the cavity does not detach from the body at the minimum pressure point but behind a laminar separation even in largely developed cavitating flow.

In the absence of laminar separation nuclei embedded in surface irregularities can promote the inception of the cavity. In that case the surface roughness (Zhang *et al*., 1998, Guennoun, 2006) is a major parameter that controls the development of the cavity.

On the other hand, some researches have been carried out to investigate the closure region of attached cavitation and the mechanism of cloud cavitation generation characterized by periodic shedding of cloud accompanying strong vibration, noise and erosion. Furness and Hutton (1975), de Lange *et al*. (1994) and Kawanami *et al*. (1997) mentioned that a re-entrant jet is the principal mechanism of cloud cavitation. The last authors proposed an investigation of the generation mechanism by controlling cloud cavitation with an obstacle fitted on the foil surface and showed that a small obstacle attached at the mid span near the closure of the sheet cavity was able to hold back the re-entrant jet, thereby preventing the generation of cloud cavitation. Note that the shedding process of large sections of the

cavity has puzzled researchers for quite a while (Gopalan and Katz, 2000) and it has been argued that the shedding is caused by a re-entrant jet, a reverse flow that forms below the cavity and pinches it intermittently. Avellan *et al*. (1988) proposed that transition of boundary layer and growth of instability on cavity surface generate cloud cavitation. Callenaere *et al*. (1998) mentioned that for the thin cavity there can be a situation where adverse pressure gradients are too weak to promote a re-entrant jet.

Moreover, surprisingly, even if different effects, like increase of lift (Dupont, 1991) observed at the beginning of cavitation development, that must be linked with wall flow modifications, very few data exist concerning the modifications introduced in the boundary layer characteristics in the wake of the cavity. This fact is probably linked with the experimental difficulties that arise when velocity measurements must be performed in bubbly mixtures.

Concerning a non conventional hydrodynamic behaviour of hydrofoil due to the attached cavitation, Kjeldsen *et al*. (2000) have been reported an increase of the pressure difference, between the faces of the foil which reach a maximum (peak) for a cavition index σ=1.1. The authors correlate this effect to a more rapid decrease of pressure on the suction side than on the corresponding pressure on the opposite side but they focus on the point that "the exact physics behind the measured pressure difference has not been completely resolved".

The physics of this phenomenon is likely the same which lay under the observation of Dupont (1991). Nevertheless, Kato *et al*. (1989) have shown that the ratio of the lift and drag parameters could also increase in such circumstances

All these results demonstrate that there is a need of experimental contribution of the boundary layer pattern in order to quantify the mechanism of attachment and closure region of attached cavity but also the modification of the liquid flow structures due to the presence of attached cavity. The double interaction between the flow and cavity structures can be responsible of the discrepancy concerning this phenomenon. In this way, Gopalan and Katz (2000) have performed experimental study to resolve the flow structure around and downstream of sheet cavitation. Using PIV technique to map instantaneous and mean flow, turbulence and vorticity, they provided the evidence that collapse of the cavities is a primary source of vorticity and that small change in the size of the cavity cause substantial increase in the turbulence level and momentum thickness in the boundary layer downstream.

This non exhaustive overview shows the major interest of the influence of the flow pattern on the cavity inception and development, but the modification of the turbulent flow structure due to the presence of the dispersed phase were not investigated in details excepted more recently by Gopalan and Katz. Nevertheless, hydrodynamicists who work on several bubbly flows have studied the induced bubble effects on the structure of the turbulent boundary layer over a flat plate or in shear or mixing layers. For example, in the two phase mixing layer, Roig *et al*.(1993) pointed out the modification of the velocity of the liquid phase due to the bubbles leading to an expansion of the mixing layer and a noticeable modification of the turbulent properties of the flow. Climent and Magnaudet (1998) analysed, with a numerical approach, the bubble motion and the induced effects on the vortex structure in the mixing layer. They highlighted the role of the residence time of bubbles in the vortex core and the influence of the bubbles accumulation in the vortex. Sridhar and Katz (1999) showed experimentally under certain conditions, even with few entrained bubbles at very low fraction, that the core of laminar, transitional and turbulent vortices is elongated and distorted. In the bubbly turbulent boundary layer over a flat plate, Wang (1985), Kato *et al*. (1999) and Gabillet *et al*. (2002) took into evidence the mechanism of momentum exchange between the two phases linked to the bubble distribution in the near wall region and showed the contribution of the fluid lightening on the wall shear stress. Djéridi *et al*. (2004) observed in a two phase Couette Taylor flow an early indication of turbulence development due to the introduction of a dispersed (non-condensable or condensable) phase.

The present study concerns our effort to resolve the flow structure around and downstream the attached cavity using refined LDV measurements of velocity components and hydrodynamic forces. In our case, we have decided to realize our experiments in presence of a stable, rather small, cavity and for such conditions the number and the size of the bubbles in the cavity wake is small enough to allow accurate measurements. To compare our results with the scientific literature we have also chosen a documented NACA0015 foil section for which extensive data base have been constituted. The focus of this study is placed on the systematic comparison of the mean and turbulent flow properties of the boundary layer with and without cavity in order to identify the modifications of the turbulent structure and global parameters of the boundary layer, upstream, around and downstream the sheet cavity.

EXPERIMENTAL SETUP

Experiments have been conducted in the cavitation tunnel of the French Naval Academy. This facility is fitted with a 1 m long and 0.192 x 0.192 m^2 square cross test section in which velocities up to 15 ms^{-1} can be achieved. Measurements realized in an empty test section have shown that the natural turbulence intensity in the test section remains lower than 3%. Instrumentation of the tunnel allows the measurement of the cavitation index $\sigma = \dfrac{p - p_v}{0.5\,\rho U_f{}^2}$. From velocity measurements determined with an accuracy of 0.75% and pressure measurements determined with an accuracy of 1.5% the cavitation index is determined with an accuracy of 3%.

The measurements are conducted on the profile for an inflow velocity U_{ref}=5 ms^{-1} at an angle of attack α=10°. In cavitating conditions the cavitation index is set

to 2.35 corresponding to $\frac{\sigma}{2\alpha} = 6.76$. This choice of the cavitation index has been guided by the length and stability of the sheet cavity that was necessary to perform velocity measurements in its wake.

The pattern of the cavity is shown figure 1. To asses for Reynolds effects measurements conducted at U_{ref} = 10 ms^{-1} are occasionally presented. For cavitating configuration the cavity has a length of $\frac{l}{c} \approx 0.2$ where l is the length of the cavity and c the chord length of the foil.

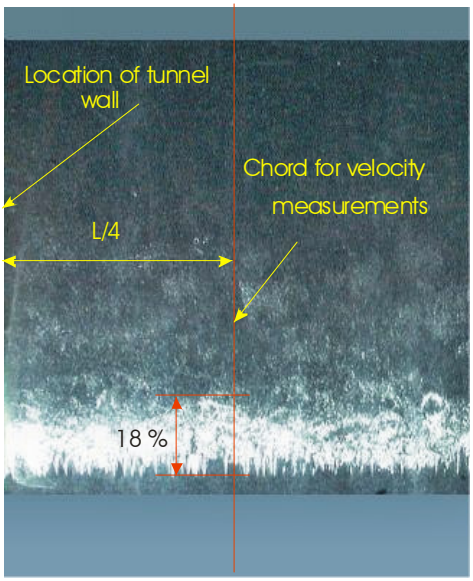

(a)

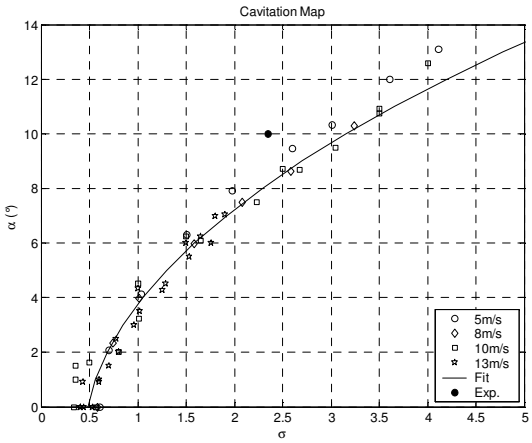

(b)

Fig. 1: Sheet cavity (a) and cavitation diagram (b)of NACA0015 foil. The plain circle (α=10°, σ=2.35) indicates the configuration used during measurements.

Measurements using the two components LDV technique are carried out on lines normal to the hydrofoil surface for different positions x/c spaced of 10% in the wake of the cavity, figure 2, and concern two components (normal and tangential) of the velocity. For our measuring setup the measuring volume has a length of 400 µm in the spanwise direction and a radius of 50 µm. The grid, refined in the near wall area (50 µm between grid points), allows the determination of the mean velocity gradient with a good accuracy. The grid represents 15 normal lines from the leading edge to the trailing edge with about 70 points per line. To determine the laminar/turbulent transition with an accuracy of 2% of x/c the grid has been refined locally in x direction. Stations have been added in the wake of the foil.

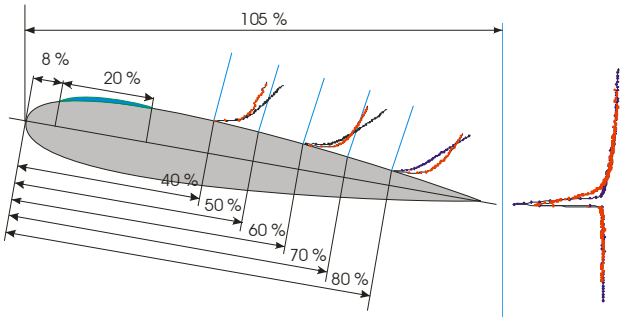

Fig. 2 : Measuring configuration in the wake of the cavity (measures are realized on the blue lines).

VELOCITY MEASUREMENTS AND INTEGRAL QUANTITIES

Boundary layer pattern in non-cavitating case:

For each point of measure 20 000 samples have been validated during a maximum of 60 s (corresponding to the near wall locations). This has been proven sufficient after having performed successive tests to measure the mean and the rms values of the u and v velocity components with a very good convergence and repetitiveness of the processing. Moreover, to evaluate the velocity bias due to the possible presence of micro-bubbles in the cavity wake, a series of test intended to distinguish bubbles from particles as been performed. Indeed, the procedure, derived from the one initially proposed by J.L. Marié (1983) and Vassalo *et al.* (1993), aiming the suppression of signal coming from particles embedded in two-phase bubbly flows has been applied. According to the previous refined grid, a survey of the distribution of mean tangential and normal velocity components is presented. Firstly, our goal was to characterise the boundary shape parameters on a Naca0015 hydrofoil. Velocity profiles were numerically integrated to compute the displacement, δ_1, momentum, δ_2 and energy, δ_3, thicknesses from which shape factors H_{12} and H_{23} are deduced. The following formulas are applied:

$$\delta_1 = \int_0^{\delta} (1 - \frac{u}{U_e}) dy \qquad \delta_2 = \int_0^{\delta} (1 - \frac{u}{U_e}) \frac{u}{U_e} dy$$

$$\delta_3 = \int_0^{\delta} (1 - \frac{u^2}{U_e^2}) \frac{u}{U_e} dy$$

$$H_{12} = \frac{\delta_1}{\delta_2} \qquad H_{23} = \frac{\delta_2}{\delta_3}$$

U_e represents the external velocity on the normal line. In our case this velocity is the maximum velocity measured at the location.

On figure 3 the dimensional velocity profiles are presented the classical velocity defect in the vicinity of the wall can be observed and the evolution of the external velocity linked with the velocity gradient is also observable.

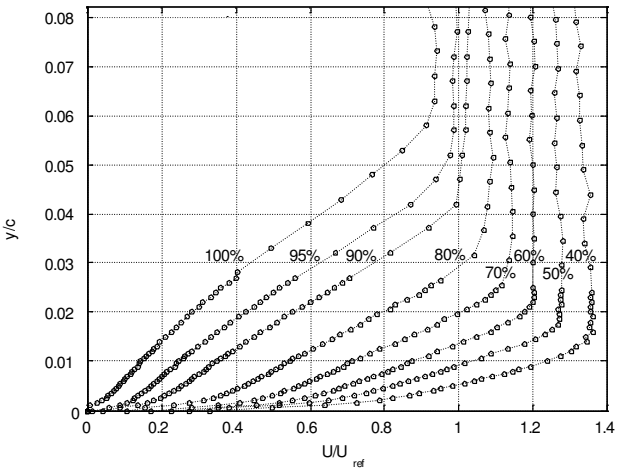

Fig. 3: Dimensional velocity profiles,
$\alpha = 10°$, $U_{ref} = 5\ ms^{-1}$, $Re = 5\ 10^5$.

Integration of the velocity profiles using the previous formulas allows the construction of the curves presented on figure 4 and 5. On figure 4 the rapid increase of the displacement thickness near the trailing edge indicates the approach of detachment. This fact is confirmed by the value of the shape factor presented on figure 5. The increase of the Reynolds number reduces the shape factor delaying the detachment. Near the leading edge the shape factor increases rapidly in the laminar boundary layer and decreases abruptly with the transition. It can be noticed that the increase of the Reynolds number from $5\ 10^5$ to 10^6 moves the transition closer to the leading edge. Moreover, after the transition the value of this parameter remain nearly constant at a value of 1.5 for a Reynolds number of $5\ 10^5$ and 1.4 for a Reynolds number of 106. This difference indicates that, for the lower Reynolds number, the boundary layer has not reached its equilibrium state. For the higher Reynolds number the classical value of 1.4 indicates a more stabilized boundary layer.

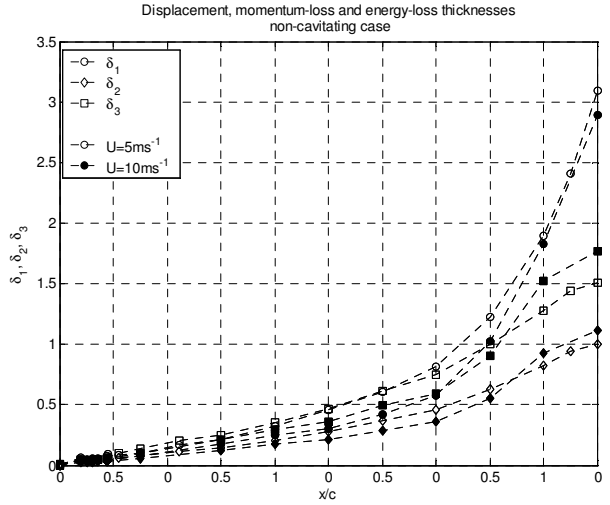

Fig. 4: Displacement, momentum and energy thicknesses for non cavitating conditions.

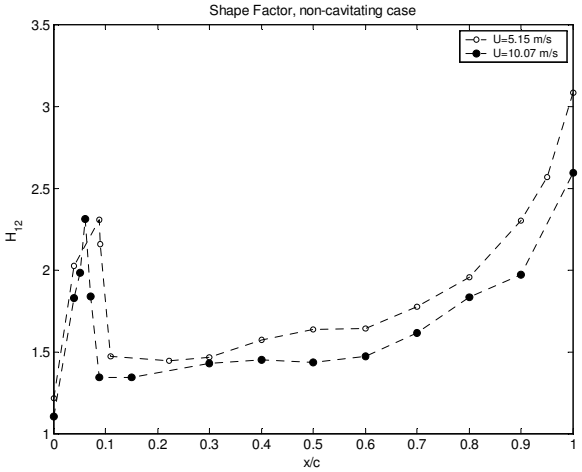

Fig. 5: Shape factor for non cavitating conditions.

To present the data closed to the wall in a classical way the following scaling is adopted:

$$u^+ = A\log\left(y^+\right) + B \text{ with } y^+ = \frac{yu^*}{\nu}$$

where $u^* = U_e\sqrt{\frac{C_f}{2}} = \sqrt{\frac{\tau_w}{\rho}}$. In these expressions C_f represents the local friction coefficient at the wall and τ_w the wall shearing stress. The determination of the friction is then necessary to apply this formulation.

The friction has been determined experimentally and numerically. Experimentally the shear stress can be determined from the measurement of the velocity gradient normal to the wall. As this measurement is rather difficult we have also used an experimental model based on the value of the integral quantities proposed by Ludwieg and Tillmann in 1950:

$$C_f = 0.246\frac{Re_{\delta_2}^{-0.268}}{10^{0.678\,H_{12}}}$$

Moreover, these values have been compared with numerical results obtained by boundary layer code 3C3D. The three curves plotted on figure 6, collapse very well in the turbulent boundary layer. Note that the transition from laminar to turbulent is poorly predicted by the code. For purpose of comparison the skin friction without pressure gradient (flat plate) has been added. It can be seen that the pressure gradient decrease the skin friction leading to the separation of the boundary layer for $C_f = 0$, just at the trailing edge in our case.

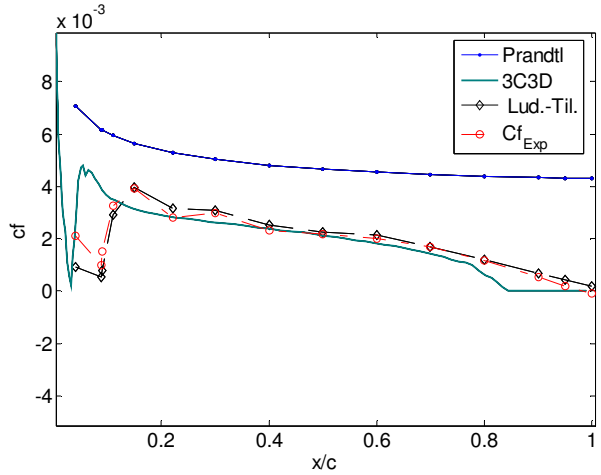

Fig. 6: Skin friction for non cavitating conditions, NACA 0015, $\alpha = 10°$, $U_{ref} = 5$ ms^{-1}.

With this previous representation the velocity profile exhibits a logarithmic behaviour for y^+ comprised between 20 and 200. The velocity distributions are represented on figure 7 using scaling law. It can be seen that the slopes of the profiles in the logarithmic area, table 1, are quite far from the classical value, 5.6, obtained for turbulent boundary layers. This is a second indication of a non equilibrium boundary layer. For the data obtained at 10 ms^{-1} values of A are close to the classical value.

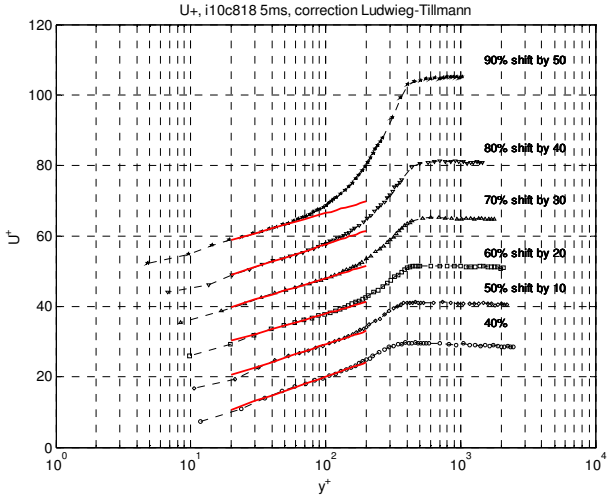

Fig. 7: Adimensionalized velocity profile using wall scaling, non cavitating conditions.

Table 1: Slopes in the logarithmic area, Non cavitating conditions.

	A (5 ms-1)	A (10 ms-1)
90 %	11.0	-
80 %	11.5	5.01
70 %	10.6	4.82
60 %	10.0	4.01
50 %	11.0	5.89
40 %	10.9	4.32

Boundary layer pattern with attached cavity:

The same measurements have been realized for cavitating conditions. Dimensional velocity profiles are presented on figure 8.

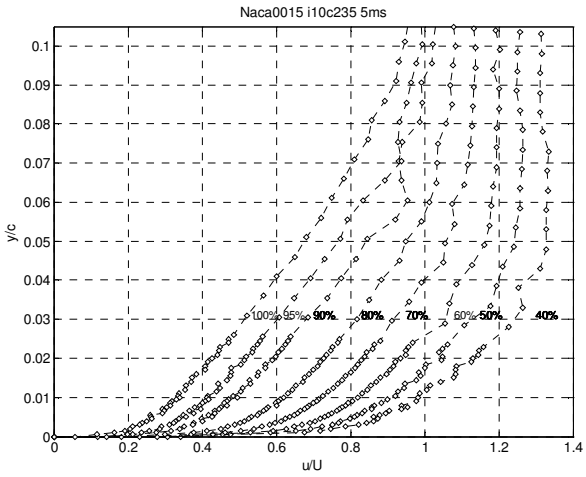

Fig. 8: Dimensional velocity profiles in cavitating case, $\alpha = 10°$, $U_{ref} = 5$ ms^{-1}, Re = 5 10^5.

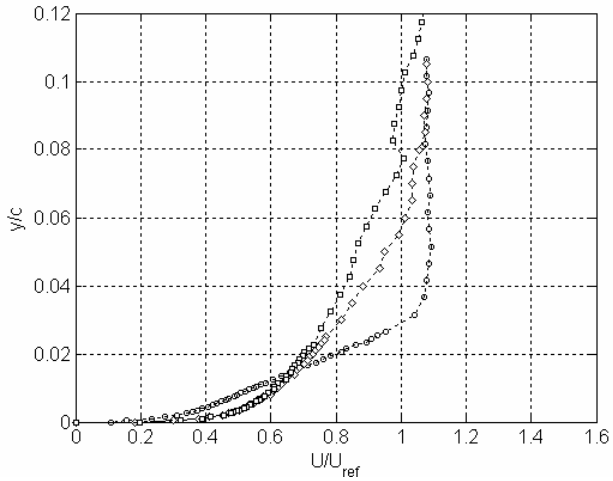

Fig. 9: Comparison of velocity profiles in the wake of the cavity, x/c =0.8,
○: non cavitating case, ◇: σ=2.35, □: σ=2.15.

It can be seen by comparison to figure 3 that the area affected by the velocity defect seems larger, it is evident on figure 9 where the velocity profiles in cavitating and non cavitating conditions are compared. Moreover, in the cavitating case the velocity in the inner region is larger than in the non cavitating case leading to a increase of the gradient at the wall and thus must lead to an increase of the skin friction. From these profiles the thicknesses and the shape factor have been determined and plotted on figures 10 and 11 respectively.

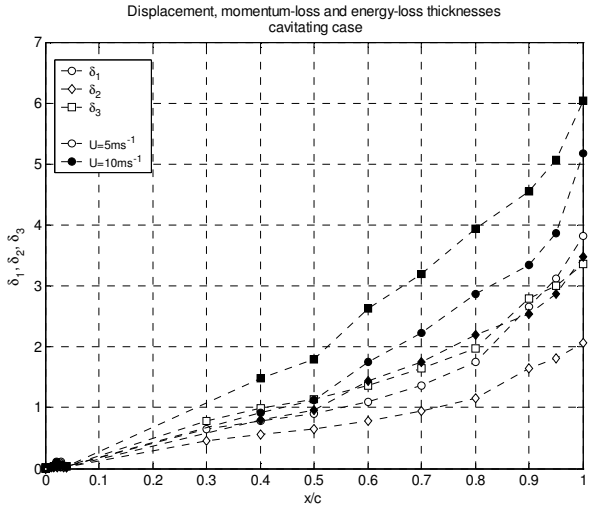

Fig. 10: Displacement, momentum and energy thicknesses, for cavitating conditions.

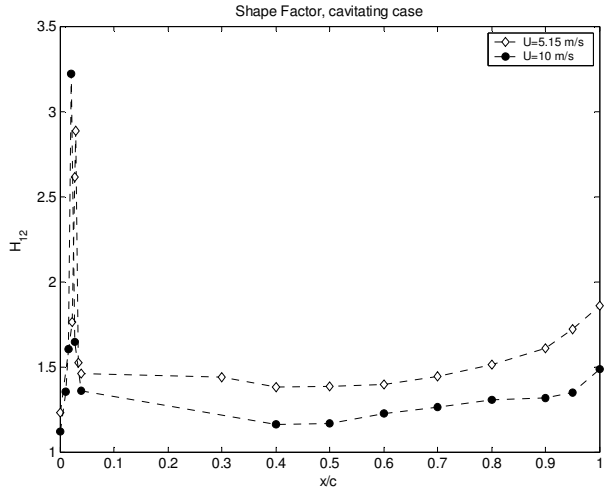

Fig. 11: Shape factor for cavitating conditions.

A comparison of the shape factor in the cavitating and non cavitating case shows that the increase of the shape factor in the laminar area is extremely rapid in the cavitating case indicating that the presence of the cavity induces a laminar detachment just in front of the cavity. The value of the shape factor in the non cavitating case is too low to conduct to the laminar detachment thus the cavity develops from surface attachment as described by Guennoun 2006 and induces the laminar separation of the boundary layer. The transition occurs and after the reattachment the boundary layer is fully turbulent with coherent value of the global parameters.

As in the non cavitating case the skin friction has been determined both experimentally and numerically. The same procedures have been used experimentally. Numerically the first step has been conducted using a CFD code in cavitation conditions then the pressure and velocity fields have been introduced in a boundary layer code (Wilcox) to determine the velocity profile in the boundary layer. The problem lies in the fact that the boundary layer code do not account for the two phase flow in the wake of the cavity but taking into account the computed pressure law, the velocity gradient is then modified and occurs as the predominant effect in the modification of the skin friction. Results are presented on figure 12 where numerical and experimental data are plotted together.

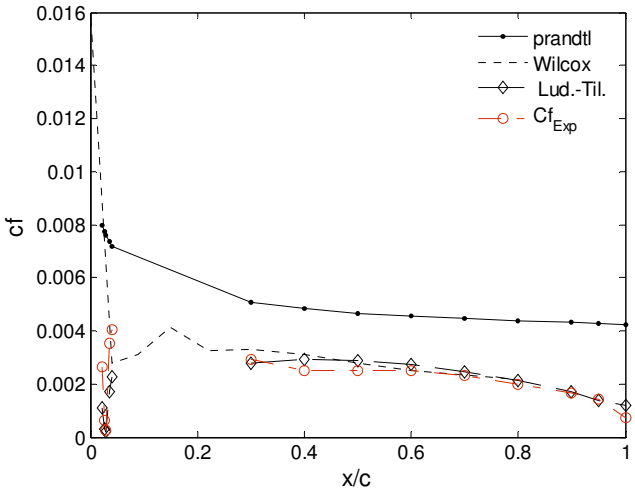

Fig. 12: Skin friction for cavitating conditions, NACA 0015, $\alpha = 10°$, $U_{ref} = 5$ ms^{-1}.

The comparison of the friction coefficients for cavitating and non cavitating conditions confirms, figure 13, that cavitation increases the friction as indicated by the velocity gradient at the wall shown on figure 9.

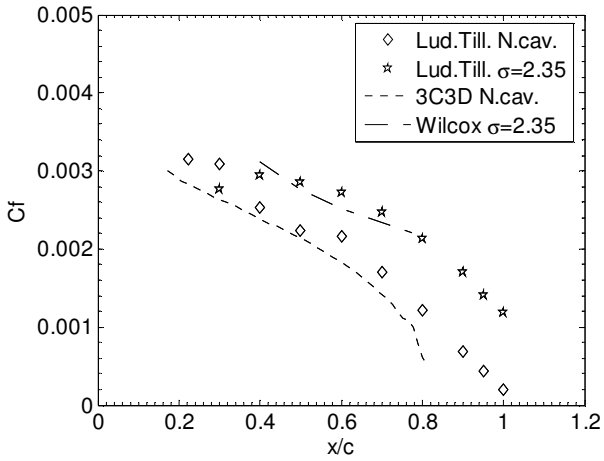

Fig. 13: Comparison of skin friction determined for: ◇: non cavitating and ★: σ=2.35 cavitating conditions.

The velocity distributions have been reported using the inner variables on figure 14. It can be seen that the general shape of the velocity profiles remains unchanged but the slope of the profile in the log area has been reduced and is now of the order of magnitude of the classical value. It seems thus that the cavitation has promoted the transition and stabilized the turbulent boundary layer which is now in equilibrium conditions as attested by the values of the slopes reported in table 2. Compared with distributions in non-cavitating case (figure 7), in the boundary layer edge, the law of the wake is reduced by the presence of the cavity and the log area is more extended. The global extend of the boundary

layer reaches y^+=3000 instead of y^+=400, in the non-cavitating case.

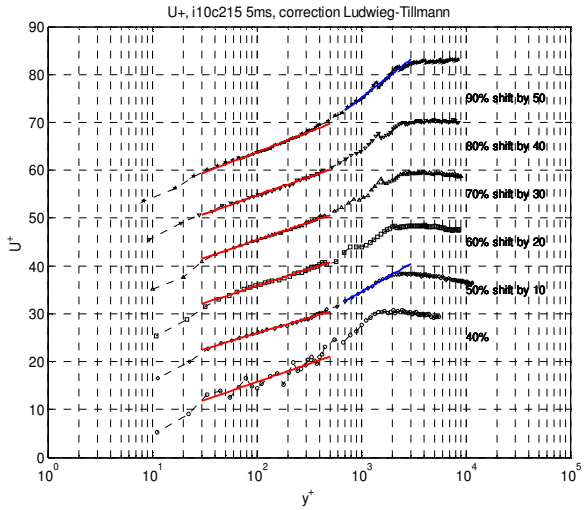

Fig. 14: Adimensionalized velocity profile using wall scaling, cavitating conditions.

Table 2: Slopes in the logarithmic area, Cavitating conditions.

	A (5 ms-1)
90 %	7.6
80 %	7.5
70 %	6.9
60 %	6.9
50 %	7.2
40 %	6.7

For boundary layers that develop in presence of a pressure gradient Truckenbrodt (Schlichting and Kestin, 1979) has proposed a correlation between the two shape factors H_{12} and H_{23} valid for attached boundary layers:

$$H_{12} = 1 + 1.48\left(2 - \frac{1}{H_{23}}\right) + 104\left(2 - \frac{1}{H_{23}}\right)^{6.7}$$

These results are presented on figures 15 and 16 for the non cavitating and cavitating cases respectively. It can be seen that the cavitation has no effect on this correlation which remains very well established in the wake of the cavity. Nevertheless, taking into account that the equilibrium of the boundary layer is more prononced in cavitating case, the good collapse of experimental data with the model is not surprising.

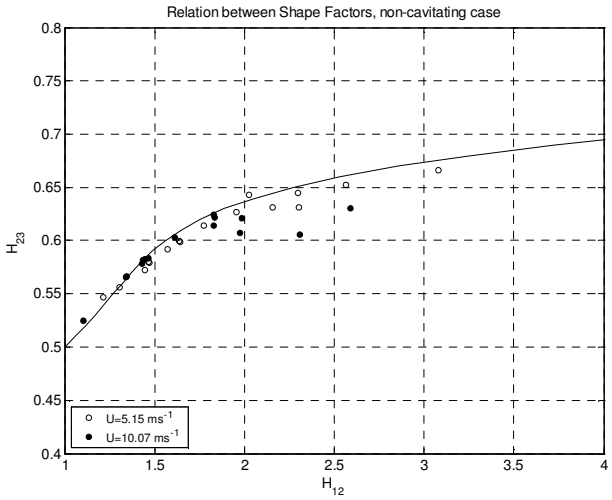

Fig. 15: Truckenbrodt correlation and experimental data, non cavitating conditions.

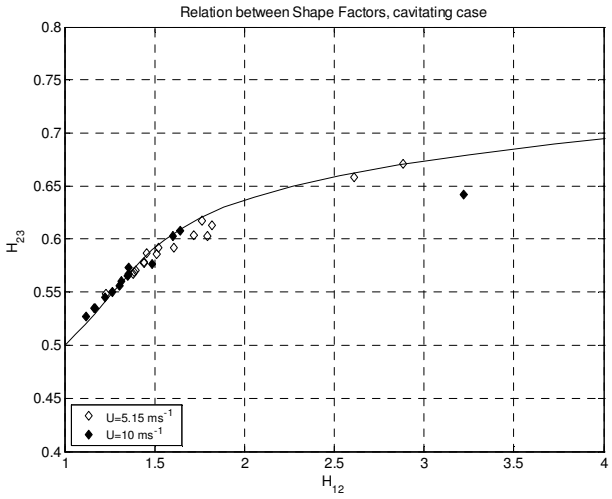

Fig. 16: Truckenbrodt correlation and experimental data, cavitating conditions.

CONCLUSIONS

The present experimental study provides the comparison of the boundary layer pattern with and without an attached stable cavity on the Naca0015 foil for Re = 510^5 and angle of attack of 10°. A refined measurements of mean velocity using LDV technique have been used in order to determine the integral quantities, shape factor and velocity distributions. A particular attention was paied on the stability of the closure region of the cavity in order to avoid a bubbly flow in the wake of the cavity and then the bias effects on the measurements of the liquid velocity. The systematic comparisons of the global parameters provide a modification of the structure of the boundary layer. In the inner region, near the wall, the presence of the cavity increases the mean tangential velocity, from x/c=0.5 to the trailing edge, leading to an increase of the velocity gradient. The comparison of the two shape factors show an ealier transition from laminar to turbulent boundary layer due to the presence of the cavity and a delay of the

separation near the trailing edge. The boundary layer in the cavitating case is larger and the shape factor plateau value tends to classical one equal to 1.4. Comparison of the velocity distributions using inner coodinates provides a stabilization of the boundary layer inducing the self similarity of the log-area. As conclusion, the presence of the cavity influence the boundary layer structure even near the trailing edge far from the closure of the cavity and the pressure distribution is modified all over the chord length. According to the cavitation index and the stable aspect of the cavity, the two phase flow aspect in the wake of the cavity has little influence on the liquid velocity. Nevertheless, taking into account the low Reynolds numbers effects, the stabilization is classically associated with a fully develloped turbulence mechanism. In the wake of the cavity, the physical mechanisms responsible to the modification of the flow pattern are not only due to the pressure distribution but also to transfert mechanism of the fluctuating part of the velocity field. Further measurements of the turbulent quantities for larger Reynolds number and lower cavitation index, are in progress in order to explain this physical mechanism.

AKNOWLEGMENT

The authors would like to express their gratitude to Robert Houdeville of ONERA for 3C3D code support.

REFERENCES

Arakeri V.H., Acosta A.J., 1973, Viscous effects in the inception of cavitation on axisymmetric bodies, Trans. ASME: Journal of Fluids Engineering, vol 95, pp 519-527.

Avellan F., Dupont P.,Rhyming I., 1988, generation mechanism and dynamics of cavitation vorticies downstream of a fixed leading edge cavity, 17th symposium on Naval Hydrodynamics, pp 317-329.

Callenaere M., Franc J-P., Michel J-M., 1998, Influence of cavity thickness and pressure gradient on the unsteady behaviour of partial cavities, 3rd International Symposium on Cavitation, Grenoble, France, April 7-10.

Climent E., Magnaudet J., 1998, Modifications d'une couche de mélange verticale induites par la présence de bulles, C. R. Acad. Sci. Paris, t. 326, Série II b, p 627-634.

de Lange D.F., de Bruin G.J., van Wijngaarden L., 1994, On the mechanism of cloud cavitation – experiments and modelling, 2nd International syposium on cavitation (Cav94) pp 45-50.

Djeridi H., Gabillet C., Billard J.Y., 2004, Two phase Couette Taylor flow: arrangement of dispersed phase and effects on the flow structures, Physics of Fluid, vol 16, n°1, pp 128-139.

Dupont P., 1991, "Etude de la dynamique d'une poche de cavitation partielle en vue de la prédiction de l'érosion dans les turbomachines hydrauliques", Thèse de l'Ecole Polytechnique Fédérale de Lausanne n° 931.

Franc J.-P., Avellan F., Belahadji B., Billard J.Y., Briançon-Marjollet L., Fréchou D., Fruman D.H., Karimi A., Kueny J.L., Michel J.M., 1995, La Cavitation. Mécanismes industriels et aspects industriels, , Collection Grenoble Sciences - ISBN 2-86883-451-5.

Franc J.P., Michel J.M., 1985. - Attached cavitation and the boundary layer: experimental investigation and numerical treatment – *Jounal of fluid mechanics, vol 154, pp 63-90.*

Furness R. A., Hutton S.P., 1975, Experimental and theoretical studies of two dimensionnal fixed type cavities, ASME, Journal of Fluids Engineering, vol 97, n° 4, pp 515-522.

Gabillet C., Colin C., Fabre J., 2002, Expetrimental study of bubble injection in a turbulent boundary layer, International Journal of Multiphase Flow, vol 28, pp 553-578.

Gates E.M., Acosta A. J., 1978, Some effects of several free stream factors on cavitation inception on axisymmetric bodies, 12th Symp. Naval Hydrodynamics, Washington DC, pp 86-108.

Gopalan S., Katz J., 1999, Effects of entrained bubbles on the structure of vortex rings, Journal of Fluid Mechanics, vol 397, pp 171-202.

Gopalan S., Katz J., 2000, Flow structure and modeling issues in the closure region of attached cavitation, Physics of Fluids, vol 12, n° 4, pp 895-911.

Guennoun F., 2006, Etude physique de l'apparition et du développement de la cavitation sur un profil isolé, unpublished.

Kato H., Iwashina T., Miyanaga M., Yamaguchi H, 1999, "Effect of microbubbles on the structure of turbulence in a turbulent boundary layer", Journal of Marine Science and Technology, vol 4, pp 155-162.

Kato H., Miura M., Yamaguchi H., Miyanaga M., 1989, "Drag reduction by intentional cavitation", Cavitation and Multiphase Flow Forum, ASME, FED-vol. 79.

Katz J., 1984, Cavitation phenomena within regions of flow separation, Journal of Fluid Mechanics, vol 140, pp 497-536.

Kawanami Y., Kato H., Yamaguchi H., Tanimura M., Tagaya Y., 1997, Mechanism and control of cloud cavitation, Journal of Fluids Engineering, vol 119, pp 788-794.

Kjeldsen M., Arndt R. E. A., Effertz M., 2000, "Spectral characteristics of sheet/cloud cavitation", Journal of Fluid Engineering, vol 122, pp 481-487.

Leroux, J.B., Astolfi, J.A. and J.Y. Billard, 2004. - An experimental study of unsteady partial cavitation - *Jounal of fluids engineering, 126: 94-101*

Ludwieg H., Tillmann W., 1950, "Investigation of the wall-shearing stress in turbulent boundary layer", NACA Technical Memorandum n° 1285.

Marie, J.L., 1983, Investigation of two-phase bubbly flows using laser doppler anemometry, Physico Chemical Hydrodynamics 4 (2), 103-118.

Marie, JL: 1983, "Investigation of two-phase bubbly flows using laser doppler anemometry", PhysicoChemical Hydrodynamics 4 (2), 103-118.

Roig V., 1993, Zones de mélange d'écoulements diphasiques à bulles, Thèse de l'Institut National Polytechnique de Toulouse, 5 mai.

Schlichting H., Kestin J., 1979, “Boundary layer theory” 7th edition, McGraw-Hill Science/Engineering/Math.

Stutz B., Reboud J.L., 1997. “Experiments on unsteady cavitation”. Experiments in Fluids 22, pp 191-198.

Vassallo P.F., Trabold T.A., Moore W.E., Kirouac G.J., 1993, “Measurement of velocities in gas-liquid two-phase flow using laser Doppler velocimetry”. Experiments in Fluids 15, 227-230.

Wang S.K.L., 1985, Three dimensional turbulence structure measurements in air-water two phase flow, PhD Thesis, Rensselaer Polytechnic Institute Troy, New York, USA.

Zhang Y., Gopalan S., Katz J., 1998, On the flow structure and vorticity production due to sheet cavitation, Proceedings of the ASME Fluids Engineering Summer Meeting, paper n° FEDSM98-5301, June 21-25, Washington DC.